Distribution and Structure of Torus-Bearing Membranes in the Wood of *Schisandra chinensis*

Jane Roddam[1], Curtis Hansen[1], Conner Ryan[1], Tanner Smith[1], Maria Auad[2], and Roland Dute[1, 3]
[1]Department of Biological Sciences, Auburn University
101 Life Sciences Building, Auburn, AL 36849, U.S.A.
[2]Department of Chemical Engineering, Auburn University
320 Ross Hall, Auburn, AL 36849
[3]Correspondence: Roland Dute (duterol@auburn.edu)

ABSTRACT

Torus-bearing pit membranes control water movement between tracheary elements of vascular plants, while at the same time they inhibit spread of air embolisms. They are common in gymnosperms but relatively rare in angiosperms. A recent manuscript noted the presence of such membranes in *Schisandra chinensis*, a species of basal angiosperm. Building on this prior report, the present manuscript presents evidence for the presence of this membrane in four more species of the genus. The torus-bearing pit membranes are best developed between tracheids, a cell type that acts as a subsidiary conducting system to the vessel members. Detailed observations with an atomic force microscope show the torus to be deposited after formation of the subtending margo is complete.

Tracheary elements are the water-conducting cells of vascular plants (Evert, 2006). Bordered pit pairs in their walls provide a pathway by which water flows from one tracheary element to another (Pittermann *et al*., 2005). At the same time, the bordered pit pairs must inhibit movement of any air bubbles present in the conducting pathway to avoid the severing of water columns and subsequent cessation of flow (Pittermann *et al*., 2005).

Pit borders of a pit pair are separated by a pit membrane. Pit membranes associated with bordered pit pairs of tracheary elements are mostly of two types (Dute, 2015). One type, found in most gymnosperms, consists of a permeable margo with relatively large pores surrounding a central, impermeable, target-like thickening, the torus. In the absence of air bubbles, water flows through the margo pores. In the presence of air bubbles however, the pit membrane is displaced (or aspirated) such that the torus blocks one aperture and stops the spread of gas embolisms. In contrast to this system, bordered pit membranes in tracheary elements of most angiosperm species are homogeneous in that they lack a torus but have much smaller diameter pores. The smaller openings decrease water flow (relative to the situation in gymnosperms), but make passage across the membrane more difficult for air bubbles (Dute, 2015; Pittermann *et al.*, 2005).

Torus-bearing intervascular pit membranes were thought to be absent from angiosperms until Ohtani and Ishida (1978) discovered them in six species of flowering plants. These pit membranes presented a third type of anatomy in that a central, impermeable torus was surrounded by a margo with very fine pores as found in other angiosperms. Since their discovery, further work in other laboratories has increased the number of torus-bearing angiosperm species to 86 (Dute, 2015).

Looking at the systematic distribution of torus-bearing pit membranes among the genera of angiosperms (Table 3.1 Dute, 2015) clearly shows this feature to be homoplastic. This conclusion

is strengthened by the presence of multiple mechanisms of torus ontogeny in different angiosperm families (compare for example Dute and Rushing [1988] and Dute *et al.* [1990]). The most recent discovery of torus-bearing pit membranes in angiosperms is that of Sano *et al.* (2013) in *Schisandra chinensis* (Turcz.) Baill.

The aims of the present publication are to extend the observations of Sano *et al.* (2013) into the nature of the substructure of the margo and torus in *S. chinensis*, to survey other species of this genus for tori, and to survey species of the sister genus *Kadsura* (Denk and Oh, 2006) as well.

MATERIALS AND METHODS

The sampled herbarium specimens that were used in this study are listed in Table 1 [Included after Literature Cited]. A five millimeter-long piece of stem was removed from the cut base of each specimen. Such samples were prepared for observations by one of the following methods:

1. For light microscopy (LM) hand cut transverse and longitudinal samples of herbarium specimens were placed in 95% ethanol under a vacuum for two hours then left at ambient air pressure overnight. Samples were carefully infiltrated and embedded in JB-4 plastic resin over a two-day period. Some herbarium specimens were rehydrated in dH_2O overnight then dehydrated to 95 % ethanol prior to embedment in JB-4 or dehydrated to absolute ethanol and air dried and mounted for SEM (q.v. #3). Transverse and longitudinal sections of the wood were cut with a thickness of 3—8 μm using a Sorvall MT-2b ultramicrotome. Wood sections were stained with a benzoate buffered, aqueous toluidine blue O (TBO) (Ruzin, 1999). Photographs were taken either with a Nikon Biophot microscope or with a Nikon Eclipse 80 I epifluorescence microscope (using the brightfield setting) with a Qimaging Fast 1394 digital camera.
2. Wood macerations were carried out according to the procedure of Wheeler (1983). Briefly, wood slivers were put into a 1:1 mixture of hydrogen peroxide and glacial acetic acid at 60° C for three days. Next, a drop of the treated tissue was placed on a slide, the fluid replaced with dH_2O, then the addition of TBO followed by a dH_2O rinse. The stained tissue was teased to separate cells and a coverslip was added prior to viewing with a light microscope.
3. For scanning electron microscopy (SEM) branch segments of 5 mm in length were split with a razor blade to expose radial longitudinal surfaces (RLS). The segments (split surface up) were then attached to an aluminum stub with fingernail polish and sputter coated with gold vapor. Observations were made with a Zeiss EVO 50 operated at 20 kV.
4. For atomic force microscopy (AFM) of herbarium specimens, wood samples of 5 mm in length were split to expose the RLS. Samples then were attached to AFM discs using fingernail polish (Dute and Elder, 2011). AFM images were captured at 512X512 resolution using Veeco NanoScope 3D using TAP 150 tips with an amplitude set point being about 1.8 V. Nanoscope 5.3l rl was used to save height, amplitude and phase images.

Three seedlings of *S. chinensis* were purchased from Horizon Herbs (Williams, Oregon, USA). Living stem segments (2 mm diameter) were cut into five mm lengths and treated for LM, SEM and AFM. Some specimens were stripped of their bark, dried for two days, then split to expose the RLS and mounted for either SEM or AFM. Other specimens were dehydrated through absolute ethanol, infiltrated with HMDS (Nation, 1983) and air dried for either SEM or AFM. Yet other living specimens were cut into 2 X 2 pieces and preserved in 3 % glutaraldehyde in 0.05 M

phosphate buffer. Fixation was followed by dehydration to 95 % ethanol followed by JB-4 embedment, sectioning, staining and observation using LM.

RESULTS
[The referenced figures are included at the end of the article.]

Wood Anatomy of *Schisandra*

Schisandra chinensis was selected for overall anatomical study due to the presence of living material as well as to the quality and quantity of herbarium specimens. Figure 1 is a trans-section of a young, living stem portion collected during its second year of growth and preserved in ethanol. The herbarium specimens that were used consisted of narrow diameter branches, which also contained few growth rings. Cytoplasm in the wood parenchyma cells was preserved better in chemically fixed specimens than in air-dried, herbarium samples. Figure 2 provides a detailed view of cell types in wood near the vascular cambium. There are two types of wood parenchyma cells: 1) axial, which partially ensheath vessel members, and 2) ray, which as the name implies, run radially through the wood from pith to ray initial cells of the vascular cambium. Rays are narrow, typically being only one cell wide (or uniseriate) as seen in material sectioned in the tangential longitudinal plane.

There are two distinct water-conducting systems in the wood of *Schisandra*. One of them consists of vessel members stacked end to end to form vessels. Measurements of cells from macerated wood of *S. chinensis*, show vessel member size to range from 75--112.5 μm in width and 325—550 μm in length (N = 25). Vessels are dead at maturity and in cross section usually are found as solitary cells in contact with both types of parenchyma as well as with the other type of water-conducting cell, the tracheid (Fig. 2). At maturity, vessel members are dead and devoid of cytoplasm and are connected by distinctly slanted end walls containing numerous, scalariform perforations (as seen tangential longitudinal section, Fig. 3). Figures 4--6 show a scalariform perforation plate in radial longitudinal section using SEM. Figures 5 and 6 are enlargements of the area indicated with an asterisk in Fig. 4 showing how individual perforations have developed from scalariform pits.

The second water-conducting system involves tracheids. Tracheids, like vessel members, are devoid of cytoplasm at maturity. They are distinguished from vessel members by being narrower (12.5--37.5 μm) (Fig. 2) and longer (400--1500 μm, N = 25). In addition, tracheids differ from vessel members in *Schisandra* by having a thicker wall (Fig. 3). Wall chemistry is indicated in a general way by color of the bound TBO, a metachromatic dye (O'Brien *et al.*, 1964). The inner layer of the secondary wall in tracheids of *S. chinensis* stains a deep purple. This layer is distinct even in black and white photographs (Fig. 3). Such a layer is lacking from vessel members of the same wood (Fig. 3). Tracheids are found in both early wood and late wood and are imperforate; that is, they lack perforations in their walls and are dependent exclusively on pit pairs to move water from one tracheid to the next. It is on the pit membrane of such pit pairs that tori are most likely to occur.

The torus is a thickening located in the center of the pit membrane. In sectional view under the light microscope, it appears as a fusiform object, which absorbs TBO heavily, resulting in a dark blue stain (Fig. 7). In face view the torus is circular (Figs. 5, 8). Position of the torus (and of the pit membrane) generally is midway between the two apertures of a pit pair when fresh material is

processed and viewed (Fig. 7), whereas in air-dried herbarium material, the torus is often displaced (aspirated) such that it occludes one of the apertures (Fig. 9).

Since tracheid walls are rather thick, each aperture associated with a pit pair has an inner and outer surface (Fig. 7), the former is located closer to the cell lumen and the outer closer to the pit membrane and torus surface. The outer surface of the aperture tends toward a circular outline and has a diameter less than that of the torus (Fig. 8, arrow). This observation of the torus diameter being greater than the outer aperture surface diameter holds true generally, but there are exceptions as shall be seen.

Distribution of Tori within the Wood

As indicated, bordered pit pairs connecting tracheids (both in early wood and late wood) always have tori. However, pitting among cells in the wood of *Schisandra* is complex due to the different cell types that are involved. As a case in point, consider Figs. 10 and 11, which represent the same vessel member isolated by maceration. By changing the focal plane, two different longitudinal walls (surfaces) are brought into focus. With the exception of the scalariform perforation to the bottom right in Fig. 11, the other openings represent pits leading from the vessel member to different cells that encircle it. Tori are a consistent feature of intertracheary pit membranes. Tori are an inconsistent feature of pit membranes separating vessel members and tracheids. Sometimes the torus is present and appears normal with the light microscope (Fig. 12); sometimes the torus is present but in a vestigial state (Fig. 13); sometimes it is absent (Fig. 14). All other types of pit membranes in the wood lack a torus.

Figures 4 and 5 summarize visually the differences in structure and pit type of the two water-conducting systems in wood of *Schisandra*.

Structure of the Intertracheary Pit Membrane--SEM

Structure of the intertracheary (torus-bearing) pit membrane was investigated in air-dried specimens of *S. chinensis* and *S. sphenanthera* Rehder & E. H. Wilson, and in HMDS-dried specimens of *S. chinensis*.

There is a clear distinction between torus and margo components of the pit membrane. The margo of air-dried membranes shows crossed microfibrils (Fig. 15). In exceptional views of air-dried material (Fig. 16), and in typical views in HMDS-dried specimens (Figs. 17 and 18), the margo is penetrated by pores of different diameters. In some instances (Figs. 16--18) many of the large openings and tears are artifactual, induced in many cases by specimen preparation and/or by heat of the electron beam (Nguyen *et al.*, 2017).

In all instances, the torus thickening is deposited atop the microfibrils of the margo and appears impermeable (*e.g*. Fig. 16). Note that any tearing found in the margo does not extend through the torus (Figs. 17 and 18).

Structure of the Intertracheary Pit Membrane--AFM

Detailed (high resolution) images of torus-bearing pit membranes were provided by atomic force microscopy (AFM). Wood of both *S. chinensis* and *S. sphenanthera* was investigated in air-dried and HMDS-dried conditions. The least physical damage was associated with HMDS-dried membranes of *S. chinensis*, so information from those pit membranes is provided herein.

The pit membrane clearly consists of two components: the fibrillar margo and the impermeable-appearing torus. The torus pad clearly sits atop the margo, which would indicate that the former is synthesized after the latter (Figs. 19, 20).

The margo consists of multiple layers of microfibrils of different diameters (Fig. 21). The torus is deposited atop a margo layer of parallel fibrils (Fig. 19); density of these microfibrils varies from one pit membrane to the next.

Morphology of the torus surface (as seen with AFM) varies, but it is generally pustular and not smooth (*e.g*. Fig. 20). In complex examples, there appear to be three regions to the torus: 1) a modified ring of pustules encircling the edge (1 in Figs. 20, 22), 2) a relatively smooth-surfaced region within 1 (2 in Figs. 20, 22), and 3) a large cluster of distinct pustules (3 in Figs. 20, 22) in the center (and highest point) of the torus. For the most part, the torus pad consists of non-fibrillar (matrix) material, but occasionally, there is evidence that microfibrils might also participate in torus construction (Fig. 23).

Pit borders enclosing the pit membrane on either side are constructed of concentrically arranged microfibrils (Fig. 24).

Torus Distribution in Spp. of *Schisandra*

Wood of various species of *Schisandra* was searched using both SEM and LM for presence of torus-bearing pit membranes. The following species had tori in addition to *S. chinensis* (Table 1): *S. micrantha* A. C. Sm., *S. sphenanthera*, *S. sphaerandra* Stapf (Fig. 25), and *S. pubinervis* (Rehder & E. H. Wilson) R. M. K. Saunders. Wood from *S. pubinervis* contained minitori in which torus diameter did not equal or surpass that of the pit apertures (Fig. 26).

The wood from some of the herbarium specimens proved refractory to preparation for microscopy. Perhaps future work on newly dried specimens will show tori in species now marked with an "N" in Table 1.

Torus Distribution in Spp. of *Kadsura*

None of the *Kadsura* species that were investigated possessed tori (Table 1).

DISCUSSION

Bailey and Nast (1948) refer to imperforate tracheary elements as "tracheids" in the related genera of *Illicium*, *Schisandra,* and *Kadsura* and comment upon the high concentration of distinct, bordered pits in these cells. In contrast, Metcalfe & Chalk (1950) refer to the same cells in the wood of *S. chinensis* as "fibers" although they note the cells' "conspicuous bordered pits." Saunders (1997), in a review of the Schisandraceae, labels the imperforate elements as "tracheids." Carlquist's (1999) study of the wood anatomy of *Kadsura* and *Schisandra* identifies the imperforate elements as (true) tracheids, and he found, as we have in the present study, that tracheid length is much greater than that of the associated vessel members. He also found tracheid wall thickness to be greater than wall thickness of the neighboring vessels. He had already identified the elements as true tracheids in 1988. Sano *et al.* (2013), in their article on pit membranes in ancestral angiosperms, opt for the term "fiber" when discussing torus-bearing pit membranes of *S. chinensis*.

Based on the high number of well-developed, circular bordered pits on the lateral walls of these cells (*q.v*. Fig. 4, this study), we would agree that their designation as "tracheids" is appropriate. This dual system of conductive elements (tracheids and vessel members) is reminiscent of the situation encountered in wood of *Cercocarpus* spp. (Dute *et al.*, 2010). Carlquist (1988) also considers this latter genus to possess true tracheids.

Pit membrane remnants in scalariform perforations have previously been illustrated for both *Schisandra* and *Kadsura* (Carlquist, 1999) as well as for a species of *Illicium* (*I. floridanum* J. Ellis) and other genera of the basal angiosperms (q.v. discussion in the introduction of Schneider and Carlquist, 2003). This situation also is apparent in various angiosperm families and is thought to represent a symplesiomorphic feature in the flowering plants (Schneider and Carlquist, 2003).

Sano *et al.* (2011) correlate water movement in imperforate tracheary elements with conductive cells that show complete pit membranes and a larger pit diameter and greater pit density than nonconductive imperforate tracheary elements. Our AFM work provides the necessary high resolution showing undamaged pit membranes between tracheids in *Schisandra* that are of a size and density to qualify as water-conducting, although dye movement was not attempted. Carlquist (1999) and Carlquist & Schneider (2002) consider such tracheid systems as found in *Schisandra* as providing a back-up or subsidiary water-conducting system having a high degree of conductive safety compared to that of the vessel system. We would agree.

When dealing with a structure as fragile as a pit membrane, one must always be alert to the problem of artifacts, especially in SEM imaging. These structural abnormalities can be induced in various ways, for example, during splitting of the wood specimens, chemical processing of the specimens, or by heat of the electron beam (Schneider and Carlquist, 2003; Jansen *et al.*, 2008; Jansen *et al.*, 2009; Nguyen *et al.*, 2017). A case in point is provided by comparing Figs. 16—19 in the present manuscript. The first three figures are SEM images of seriously damaged pit membranes. The porosity of the margo differs vastly among them, and all three margos in turn differ from the AFM image in Fig. 19. How are investigators able to determine the real anatomy of the pit membrane *versus* artifact? In some instances (as with the heat of the electron beam), the damage to the pit membrane occurs in real time, and one can quickly associate cause and effect (Nguyen *et al.*, 2017). Jansen and associates (Jansen *et al.,* 2008; 2009; Li *et al.*, 2016) have carefully catalogued

the effects of various treatments on intervascular pit membrane structure. They have concluded, among other things, that alcohol has a "clear dehydrating effect on the samples, resulting in more porous pit membranes" (Jansen *et al.*, 2008). They were referring to SEM samples, yet material prepared for TEM is routinely passed through an alcohol or acetone series prior to embedment in resin (e.g. Dute, 1994). Alcohol is an intermediary fluid that is miscible with both the aqueous fixative solution and the hydrophobic plastic resin.

Another instance of membrane change involves air drying and pit membrane aspiration. Aspirated pit membranes are known to be thinner and denser than non-aspirated pit membranes (Dute, 1994; Pesacreta *et al.*, 2005; Li *et al.*, 2016); but even in such instances, aspiration occurring naturally to the intrtracheary pit membranes of *Gingko* wood *versus* aspiration produced by air drying leads to different sectional images using the TEM (Dute, 1994).

In truth, pit membranes are so fragile that any preparatory technique and/or microscope combination is likely to introduce artifacts of some sort. Added to this is the fact that a given research laboratory is often limited in its equipment holdings, and so it is restricted in the types of observations that it can accomplish.

Recent pit membrane studies have been carried out using field emission scanning electron microscopes. However, the atomic force microscope provides atomic level resolution (Hanley *et al.*, 1992), and the specimen avoids being coated with metal and avoids interaction with a hot electron beam (Dute & Elder, 2011). Investigation of hydrated pit membrane with the AFM has, in our opinion, the best chance of observing torus-bearing pit membranes in their natural state (Pesacreta *et al.*, 2005).

The presence of minitori in pit membranes of *S. pubinervis* is surprising. Wheeler (1983) noted that torus diameter is less than aperture diameter in *Celtis reticulata* Torr. Individual instances of this situation have been observed in other torus-bearing species (e.g. Dute *et al.*, 2004). In such cases the torus diameter would not be sufficient to provide a tight seal during aspiration. Nevertheless, such thickenings would strengthen the pit membrane at its center and prevent or reduce the likelihood of membrane tearing at that site during aspiration (Wheeler, 1983). It is unfortunate that we had but one specimen of *S. pubinervis* on which to base our observations.

A recent review (Dute, 2015) lists all known dicot species whose intervascular pit membranes possess a torus. The list includes 86 species from six families (Oleaceae, Thymelaeaceae, Rosaceae, Ulmaceae/Cannabaceae, Schisandraceae). To this list we must add 4 more species from the present study. Although occasional species might be added to this list in the future, we doubt that the numbers will increase drastically. As noted in the review, it appears as if the appearance of torus-bearing pit membranes is homoplastic at the level of the family. This hypothesis is supported by different mechanisms of torus ontogeny among the families (q.v. Dute, 2015). Sano *et al.* (2013) correctly note that their report of tori in *S. chinensis* represents the first such observation from the basal angiosperms. The other torus-bearing species are located within the eudicots. As a point of interest, a study of tracheary elements of *Amborella trichopoda* Baill. shows no evidence of torus-bearing pit membranes (Feild *et al.*, 2000). *Amborella* is considered the sister group of all other angiosperms (Feild *et al.*, *2000*).

Material of the torus thickening is deposited as a secondary wall late in pit ontogeny. In this respect, development is akin to that of *Osmanthus*, *Daphne* and *Cercocarpus* and unlike torus development in *Ulmus*, *Celtis*, conifers and *Ginkgo* (Dute, 2015).

ACKNOWLEGEMENTS

We thank directors, curators and staff of the following herbaria for kindly providing loans of specimens and material for this study: AUA, L, MO, NY, PH and US. This research was supported by an Undergraduate Research Award (to J. R.) from the Fund for Excellence of the Department of Biological Sciences, Auburn University. This is contribution no. 746 of the Auburn University Museum of Natural History.

LITERATURE CITED

Bailey, I. W., and Nast, C. G. 1948. Morphology and relationships of *Illicium*, *Schisandra*, and *Kadsura*. I. Stem and Leaf. *Journal of the Arnold Arboretum*. 29: 77--89.

Carlquist, S. 1988. Comparative wood anatomy. Springer-Verlag, Berlin, Germany.

Carlquist, S. 1999. Wood and bark anatomy of Schisandraceae: Implications for phylogeny, habit, and vessel evolution. *Aliso* 18: 45--55.

Carlquist, S. and Schneider, E. L. 2002. The tracheid-vessel element involves multiple, independent features: Cladistic consequences. *American Journal of Botany*. 89: 185--195.

Denk, T. and Oh, I-C. 2006. Phylogeny of Schisandraceae based on morphological data: evidence from modern plants and the fossil record. *Plant Systematics and Evolution*. 256: 113--145.

Dute, R. R. 1994. Pit membrane structure and development in *Ginkgo biloba*. *International Association of Wood Anatomists Journal*. 154: 75--90.

Dute, R. R. 2015. Development, structure and function of torus-margo pits in conifers, ginkgo and dicots. *In* U. Hacke [ed.], Functional and ecological xylem anatomy, 77-102. Springer International Publishing, Switzerland.

Dute, R. R., and Elder, T. 2011. Atomic force microscopy of torus-bearing pit membranes. *International Association of Wood Anatomists Journal*. 32: 415--430.

Dute, R. R., Martin, A. L., and Jansen, S. 2004. Intervascular pit membranes with tori in wood of *Planera aquatic* J. F. Gmel. *Journal of the Alabama Academy of Science*. 75: 7--21.

Dute, R., Patel, J., and Jansen, S. 2010. Torus-bearing pit membranes in *Cercocarpus*. *International Association of Wood Anatomists Journal*. 31: 53--66.

Dute, R. R., and Rushing, A. E. 1988. Notes on torus development in the wood of *Osmanthus americanus* (L.) Benth. & Hook. *ex* Gray (Oleaceae). *International Association of Wood Anatomists Bulletin, New Series*. 9: 41--51.

Dute, R. R., Rushing, A. E., and Perry, J. W. 1990. Torus structure and development in species of *Daphne. International Association of Wood Anatomists Bulletin, New Series*. 11: 401--412.

Evert, R. F. 2006. Esau's plant anatomy. Third Edition. John Wiley & Sons, Inc., Hoboken, New Jersey, USA.

Feild, T. S., Zweiniecki, M. A., Brodribb, T., Jaffré, T., Donoghue, M. J., and Holbrook, N. M. 2000. Structure and function of tracheary elements in *Amborella trichopoda*. *International Journal of Plant Sciences*. 161: 705--712.

Hanley, S. J., Giasson, J., Revol, J.-F., and Gray, D. C. 1992. Atomic force microscopy of cellulose microfibils: comparison with transmission electron microscopy. *Polymer*. 33: 4639--4642.

Jansen, S., Choat, B., and Pletsers A. 2009. Morphological variation of intervessel pit membranes and implications to xylem function in angiosperms. *American Journal of Botany*. 96: 409--419.

Jansen, S., Pletsers, A., and Sano, Y. 2008. The effect of preparation techniques on SEM-imaging of pit membranes. *International Association of Wood Anatomists Journal*. 29: 161--178.

Li, S., Lens, F., Espino, S., Karimi, Z., Klepsch, M., Schenk, H. J., Schmitt, M., Schuldt, B., and Jansen, S. 2016. Intervessel pit membrane thickness as a key determinant of embolism resistance in angiosperm xylem. *International Association of Wood Anatomists Journal*. 37: 152--171.

Metcalfe, C. R., and Chalk, L. 1950. Anatomy of dicotyledons. Clarendon Press, Oxford, United Kingdom.

Nation, J. L. 1983. A new method using hexamethyldisilazane for preparation of soft insect tissues for scanning electron microscopy. *Stain Technology* 58: 347--351.

Nguyen, C., Andrews, A., Baas, P., Bond, J. E., Auad, M., and Dute, R. R. 2017. Pit membranes and their evolution in the Oleinae of the Oleaceae. *International Association of Wood Anatomists Journal*. 38: 201--219.

O'Brien, T. P., Feder, N., and McCully, M. E. 1964. Polychromatic staining of plant cell walls by toluidine blue O. *Protoplasma*. 59: 368--373.

Ohtani, J., and Ishida, S. 1978. Pit membranes with a torus in dicotyledonous woods. *Mokuzai Gakkaishi*. 24: 673--675.

Pesacreta, T. C., Groom, L. H., and T. G. Rials, T. G. 2005. Atomic force microscopy of the intervessel pit membrane in the stem of *Sapium sebiferum* (Euphorbiaceae). *International Association of Wood Anatomists Journal*. 26: 397--426.

Pittermann, J., Sperry, J. S., Hacke, U. G., Wheeler, J.K., and Sikkma, E. H. 2005. Torus-margo pits help conifers compete with angiosperms. *Science*. 310: 1924.

Ruzin, S. E. 1999. Plant microtechnique and microscopy. Oxford University Press, New York, New York, USA.

Sano, Y., Morris, H., Shimade, H., DeCraene, L. P. R., and Jansen, S. 2011. Anatomical features associated with water transport in imperforate tracheary elements of vessel-bearing angiosperms. *Annals of Botany*. 107: 953—964.

Sano, Y., Utsumi, Y., and R. Nakada. 2013. Homoplastic occurrence of perforated pit membranes and torus-bearing pit membranes in ancestral angiosperms as observed by field-emission scanning electron microscopy. *Journal of Wood Science*. 59: 95--103.

Saunders, R. M. K. 1997. Schisandraeae. *Flora Malesiana*. Series I, 13: 185--207.

Schneider, E. L. and Carlquist, S. 2003. Perforation plate diversity in *Illicium floridanum* (Illiciaceae) with respect to organs, provenance, and microtechnical methods. *Sida*. 20: 1047--1057.

Wheeler, E. A. 1983. Intervascular pit membranes in *Ulmus* and *Celtis* native to the United States. *International Association of Wood Anatomists Bulletin*. 4: 79--88.

TABLES AND FIGURES

Table 1. Specimens of *Kadsura* and *Schisandra* used in this study. AUA = Auburn University Herbarium; L= Leiden branch of National Herbarium of the Netherlands; MO = Missouri Botanical Garden; NY = New York Botanical Garden; PH = Academy of Natural Sciences, Philadelphia; US = Smithsonian

Species	Herbarium	Date of Collection	Collector(s) No.	Torus (Y/N)
***K. coccinea* (Lem.) A.C. Sm.**	PH	10 Jun 1995	*Qi 239*	N
***K. coccinea* (Lem.) A.C. Sm.**	US	1932-1933	*Chun & Tso 44188*	N
***K. heteroclita* (Roxb.) Craib**	PH	8 Aug 1970	*Huang & Kao 5435*	N
***K. heteroclita* (Roxb.) Craib**	US	24 Aug 1970	*Hu 10888*	N
***K. scadens* Blume**	PH, US	4 Jun 1972	*Stone 10777*	N
***S. arisanensis* Hayata subsp. *viridis* (A.C. Sm.) R.M.K. Saunders**	NY	1 Aug 1932	*Tsang 21423*	N
***S. arisanensis* Hayata subsp. *viridis* (A.C. Sm.) R.M.K. Saunders**	NY		*Tsui 825*	N

***S. bicolor* W.C. Cheng**	MO	9 Aug 1963	*Chiu s.n.*	N
***S. chinensis* (Turcz.) Baill.**	MO			Y
***S. chinensis* (Turcz.) Baill.**	L		*anon. 10781*	Y
***S. chinensis* (Turcz.) Baill.**	L		*anon. 254*	Y
***S. elongata* Baill.**	PH		*Thoms. s.n.*	N
***S. elongata* Baill.**	US	1885-1888	*Henry 6383*	N
***S. glabra* (Brickell) Rehder**	AUA	2 Jul 1960	*Ahles 53722*	N
S. henryi* C.B. Clarke subsp. *henryi	NY	23 Aug 1988	*Boufford & Bartholomew 24074*	N
S. henryi* C.B. Clarke subsp. *henryi	NY	9 Jul 1985	*Yao 9514*	N
***S. lancifolia* (Rehder & E.H. Wilson) A.C. Sm.**	NY	May-Oct 1922	*Rock 4299*	N
***S. micrantha* A.C. Sm.**	NY		*Henry 11211*	Y
***S. neglecta* A.C. Sm.**	NY		*Henry 10697*	N
***S. nigra* Maxim.**	NY	13 Jul 2003	*Watanabe et al. s.n.*	N
***S. perulata* Gagnep.**	US	Apr 1925	*Tonkin s.n.*	N
***S. plena* A.C. Sm.**	NY		*A. Henry 12192*	N
***S. propinqua* (Wall.) Baill. subsp. *intermedia* (A.C. Sm.) R.M.K. Saunders**	NY		*A. Henry 13023*	N
***S. propinqua* (Wall.) Baill. subsp. *sinensis* (Oliv.) R.M.K. Saunders**	NY	18 Jun 1934	*Chow 567*	N
***S. pubescens* Hemsl. & E.H. Wilson**	NY	1928	*Fang 2632*	N
***S. pubinervis* (Rehder & E.H. Wilson) R.M.K. Saunders**	NY	21 Jul 1989	*Zhao Qing-Sheng 1069*	Y
***S. repanda* (Siebold & Zucc.) Radlk.**	US	12 Jul 1889	*Watanabe s.n.*	N
***S. sphaerandra* Stapf**	NY	7 Aug 2005	*Gaoligong Shan Biodiversity Survey 25699*	Y
***S. sphenanthera* Rehder & E.H. Wilson**	NY	1 Jun 1994	*Boufford, Liu, Ying, C. J. Zhang*	Y

			& X.C. Zhang 26380	
***S. sphenanthera* Rehder & E.H. Wilson**	NY	15 May 2007	*Boufford & Jia 37614*	Y, but uncommon
***S. sphenanthera* Rehder & E.H. Wilson**	MO	May 2005	*Wang s.n.*	Y

FIGURES REFERENCED IN RESULTS
[FIGURES ARE NUMBERED IN THE LOWER RIGHT CORNER OF EACH IMAGE]

Abbreviations used in the figures of this study. A = axial parenchyma cell; AP = aperture in pit border; B = circular pit border; IA = inner aperture; M = margo; OA = outer aperture; P = perforation plate; PH = secondary phloem; PI = pith; R = ray parenchyma (cell); T = tracheid; TO = torus; V = vessel (member); VC = vascular cambium. XY = secondary xylem or wood. All figures depict *S. chinensis* except for Figure 16, which is *S. sphenanthera*, and Figures 25 and 26, which are *S. sphaerandra* and *S. pubinervis*, respectively.

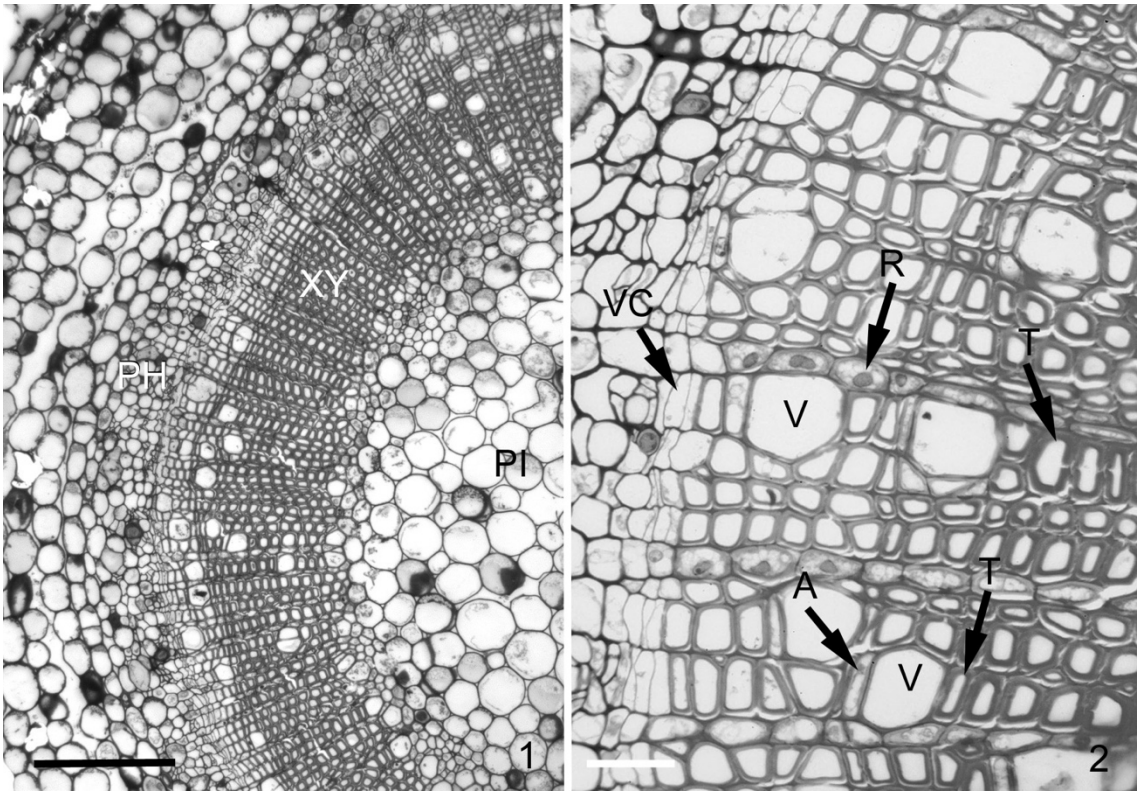

Figure 1. Trans-section of a branch showing secondary xylem and phloem. The portion of the branch was in its second year of growth when collected. **Figure 2**. A detail of the wood (secondary xylem) from Figure 1. A uniseriate ray is indicated, and vessel members and tracheids are distinguished one from the other. Scale bars = 100 µm (Fig.1) and 30 µm (Fig. 2).

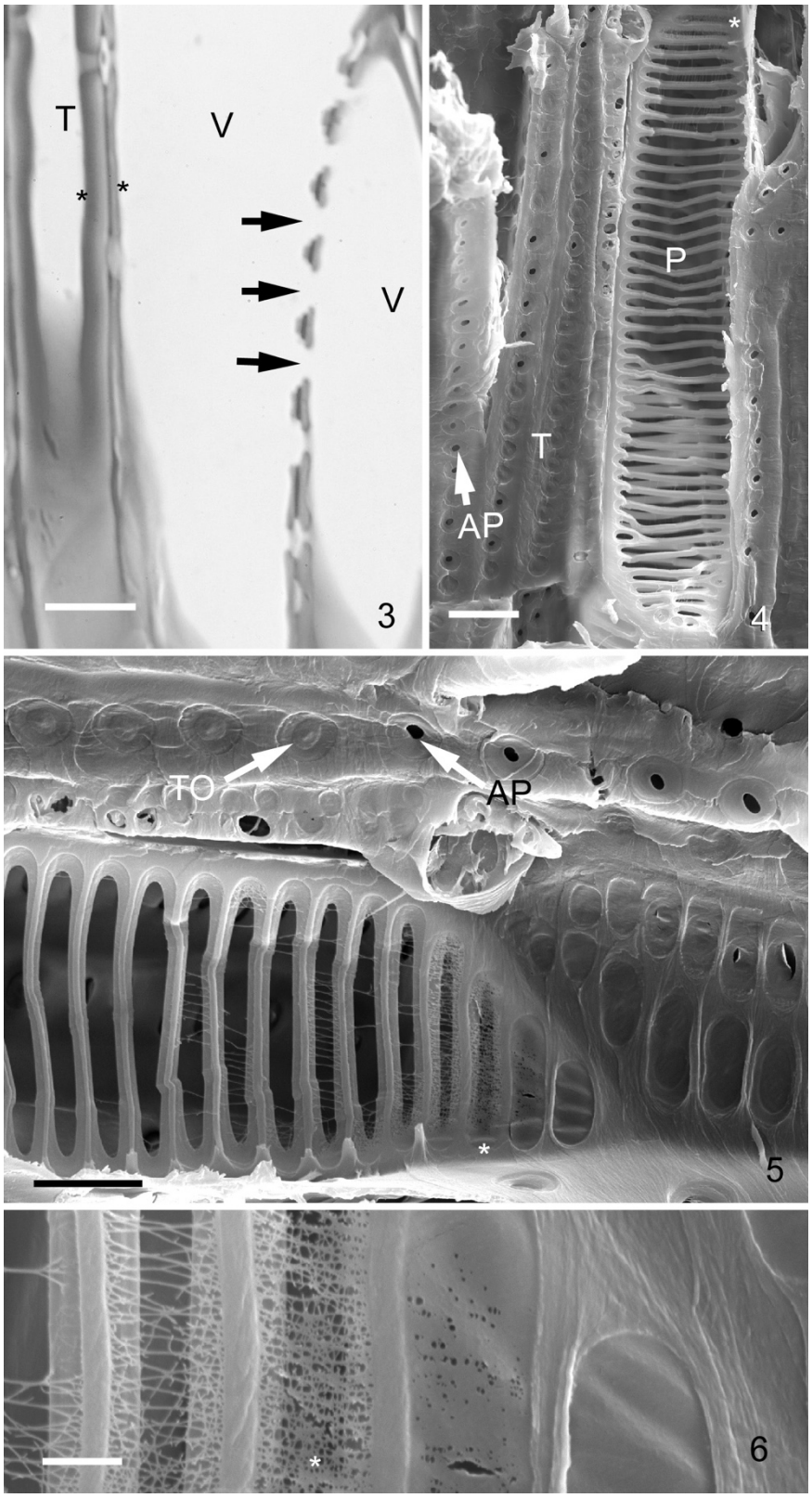

Figure 3. A perforation plate (seen in tangential longitudinal section) connecting two vessel members. Arrows indicate individual perforations. The difference between tracheids and vessel members as regards wall thickness and chemistry is evident (asterisks). **Figure 4**. A scalariform perforation plate seen in radial longitudinal section using a scanning electron microscope (SEM). The perforation plate is flanked to the left by three tracheids. Asterisks in Figures 4—6 indicate the same position in each figure. **Figure 5** is an enlargement of Figure 4 that is rotated 90º. A torus and a bordered pit aperture are denoted in a tracheid. **Figure 6** is a further enlargement of Figure 5. Note how the perforations grade into scalariform pits. Scale bars = 10 µm (Fig. 3), 10 µm (Fig. 4), 10 µm (Fig. 5) and 2 µm (Fig. 6).

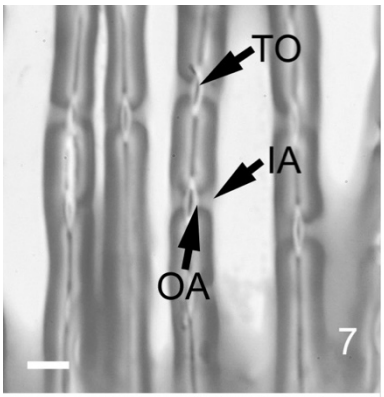

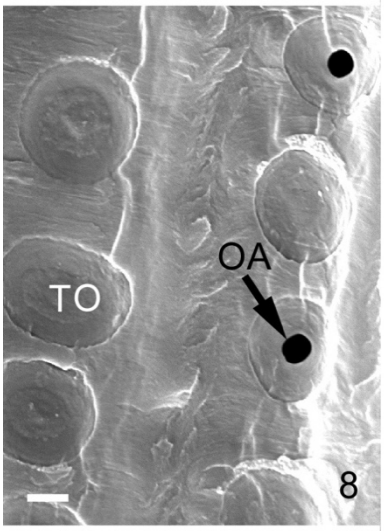

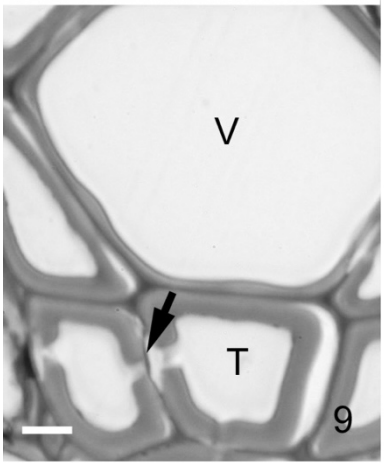

Figure 7. Light micrograph of a preserved specimen showing nonaspirated tori in sectional view. The outer *versus* inner aperture of a pit canal are indicated. Tori generally are of a greater diameter than the outer aperture. **Figure 8**. SEM of bordered pits in a tracheid wall of a herbarium specimen. In some pits the pit membrane and torus are exposed, in others, the pit membrane has been removed exposing the pit border with the outer aperture. **Figure 9**. Herbarium material in which the pit membrane is aspirated (unlabeled arrow) show how the torus completely occludes an aperture. Scale bars = 5 µm (Fig. 7), 2 µm (Fig. 8) and 5 µm (Fig. 9).

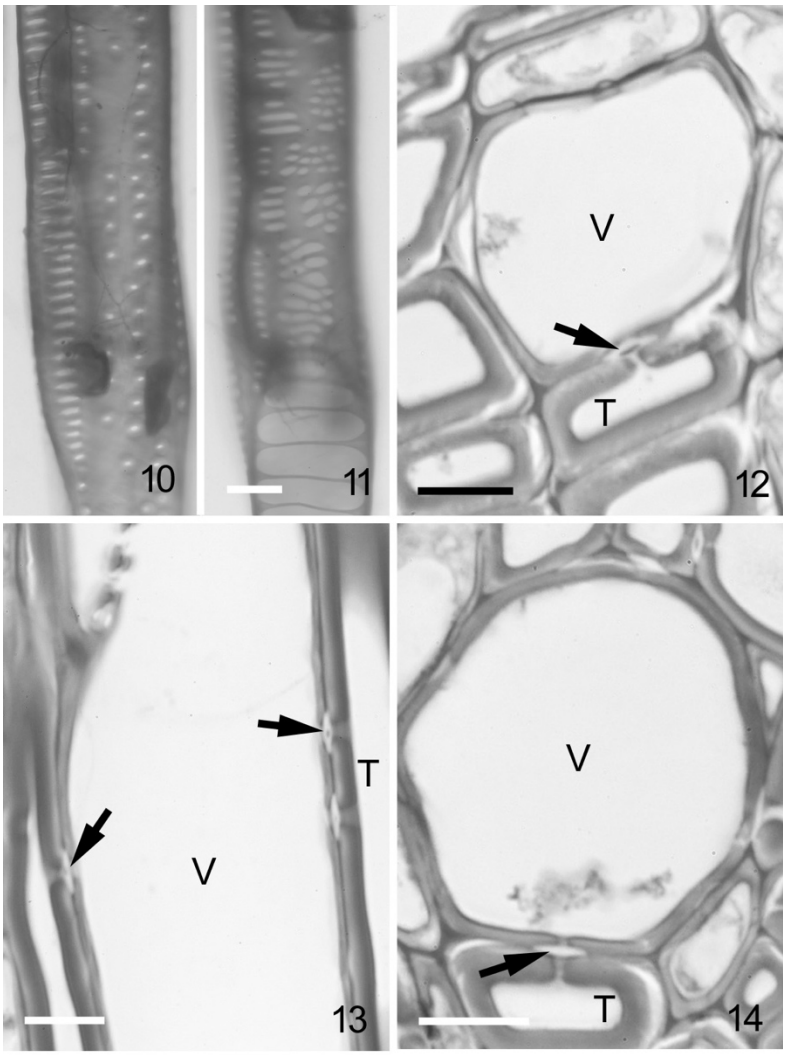

Figures 10, 11. Two focal planes of the same vessel member showing different pits on each cell surface. **Figure 12.** Wood transsection showing a well-developed torus (arrow) between a vessel member and a tracheid. **Figure 13**. A longitudinal section in which tori between vessel member and tracheids are poorly developed. **Figure 14**. A bordered pit pair between vessel member and tracheid in which the torus is absent (arrow). Scale bars = 20 µm (Figs. 10, 11), 10 µm (Fig. 12), 10 µm (Fig. 13) and 10 µm (Fig. 14).

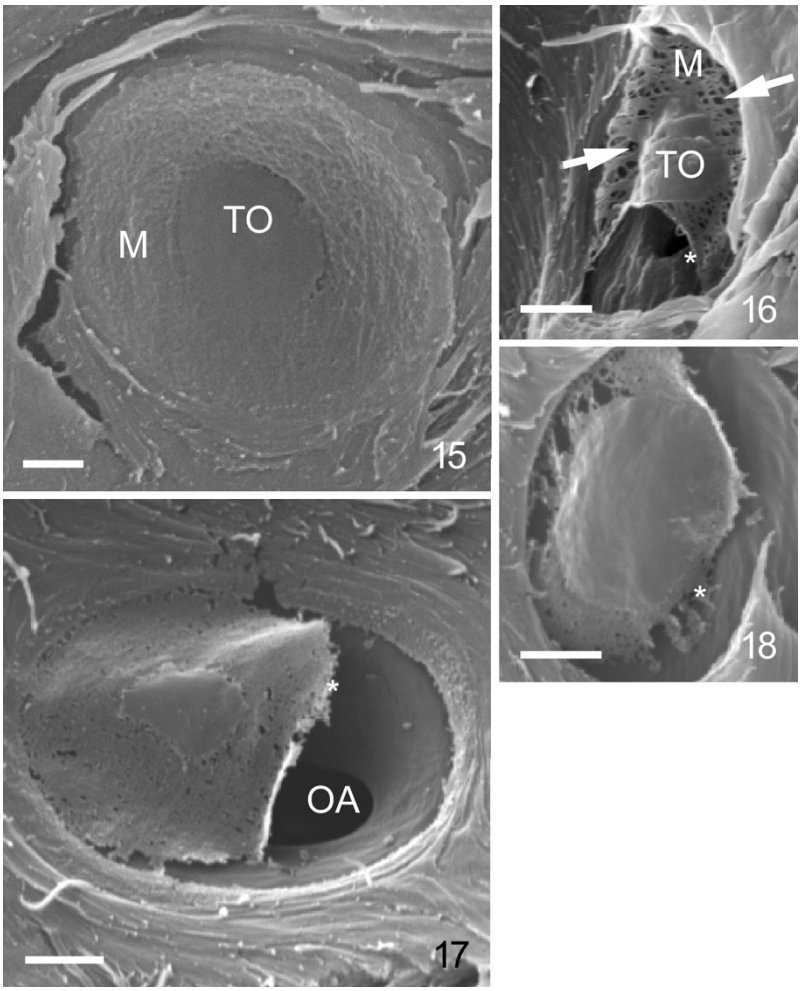

Figures 15—18. Scanning electron micrographs of torus-bearing pit membranes in *Schisandra* wood. **Figure 15**. Air-dried specimen. Note the difference in surface texture between torus and margo. The woven nature of the latter is evident. **Figure 16**. An unusual air-dried specimen in which the pit membrane is damaged, but distinct openings are present in the margo (arrows). **Figures 17 & 18**. Both pit membranes were dried with HMDS. Neither pit membrane is aspirated, but considerable damage is present in each (asterisks). Very small openings are present in the margos. Scale bars = 1 μm (Fig. 15), 1μm (Fig. 16), 1 μm (Fig. 17) and 1μm (Fig. 18).

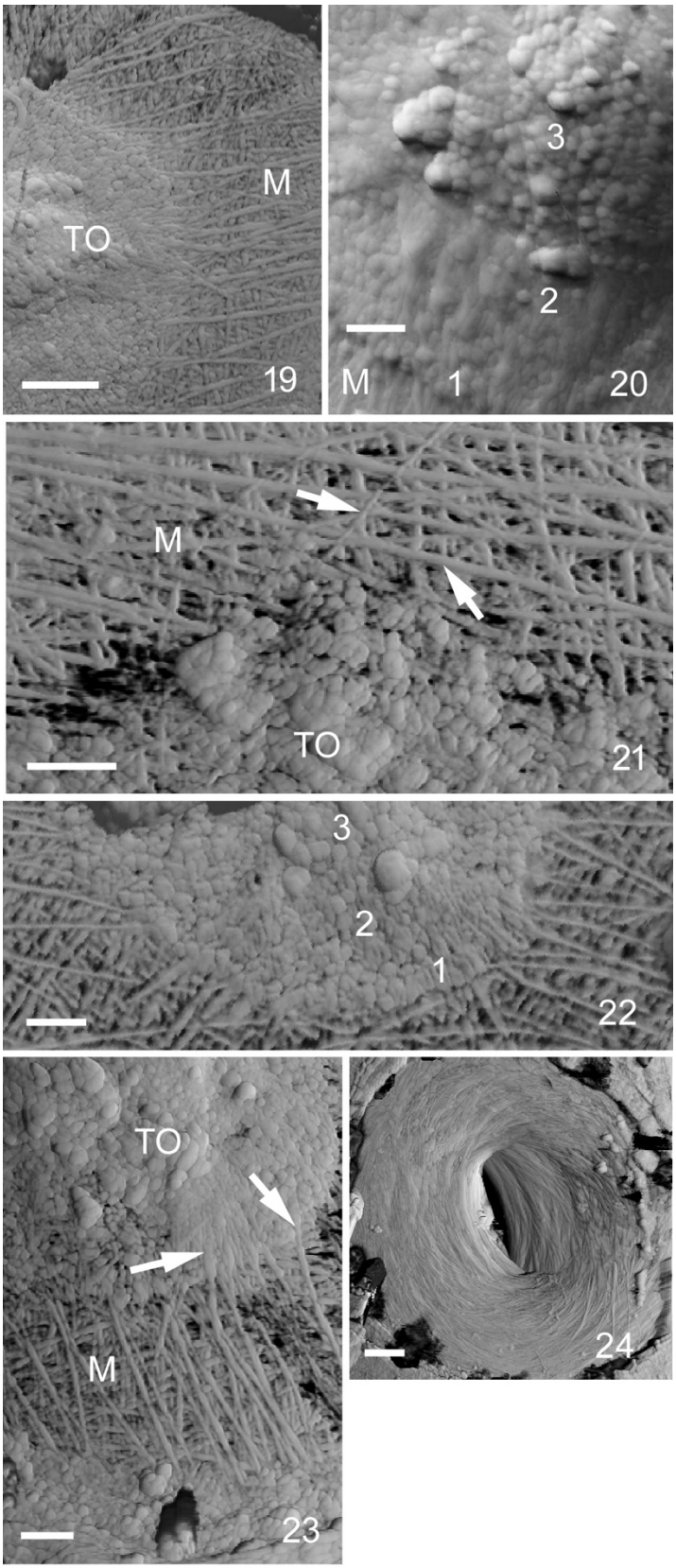

Figures 19—23 represent atomic force microscope images of torus-bearing pit membranes. **Figure 19**. An overall view of a pit membrane. Torus and margo are clearly distinct. The surface layer of the margo has microfibrils that run parallel to one another. **Figures 20 & 22** show the three regions of the torus. **Figure 21** is a detail of the pit membrane in which the margo is shown to consist of microfibrils of different diameters (arrows). The torus is clearly situated on the surface of the margo. **Figure 23.** A case in which microfibrils seem to take part in torus construction (arrows). **Figure 24**. This image reveals the fibrillar nature of the pit border. Scale bars = 0.5 µm (Fig. 19), 0.25 µm (Fig 20), 0.25 µm (Fig. 21), 0.25 µm (Fig. 22), 0.25 µm (Fig. 23) and 0.5 µm (Fig. 24).

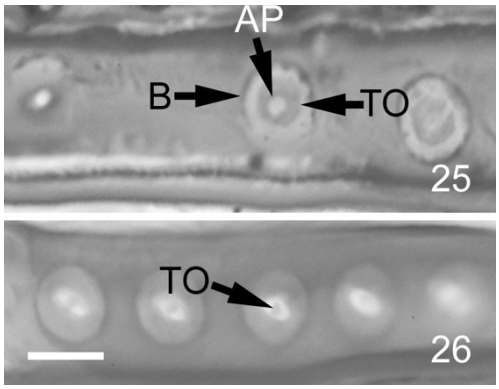

Figure 25. Circular bordered pits with distinct tori in wood of *S. sphaerandra*. **Figure 26**. Wood of *S. pubinervis* with minitori whose sizes were confirmed in trans-section. Scale bar = 5 µm (Figs. 25 and 26).